ARMY RESEARCH LABORATORY

ARL

Acoustic Detection and Tracking of a Class I UAS with a Small Tetrahedral Microphone Array

by Minas Benyamin and Geoffrey H Goldman

NOTICES

Disclaimers

Army Research Laboratory

Adelphi, MD 20783-1138

ARL-TR-7086 **September 2014**

Acoustic Detection and Tracking of a Class I UAS with a Small Tetrahedral Microphone Array

Minas Benyamin and Geoffrey H Goldman
Sensors and Electron Devices Directorate, ARL

REPORT DOCUMENTATION PAGE			*Form Approved* *OMB No. 0704-0188*	

Public reporting burden for this collection of information is estimated to average 1 hour per response, including the time for reviewing instructions, searching existing data sources, gathering and maintaining the data needed, and completing and reviewing the collection information. Send comments regarding this burden estimate or any other aspect of this collection of information, including suggestions for reducing the burden, to Department of Defense, Washington Headquarters Services, Directorate for Information Operations and Reports (0704-0188), 1215 Jefferson Davis Highway, Suite 1204, Arlington, VA 22202-4302. Respondents should be aware that notwithstanding any other provision of law, no person shall be subject to any penalty for failing to comply with a collection of information if it does not display a currently valid OMB control number.
PLEASE DO NOT RETURN YOUR FORM TO THE ABOVE ADDRESS.

1. REPORT DATE *(DD-MM-YYYY)*	2. REPORT TYPE	3. DATES COVERED (From - To)
September 2014	Final	

4. TITLE AND SUBTITLE	5a. CONTRACT NUMBER
Acoustic Detection and Tracking of a Class I UAS with a Small Tetrahedral Microphone Array	
	5b. GRANT NUMBER
	5c. PROGRAM ELEMENT NUMBER
6. AUTHOR(S)	5d. PROJECT NUMBER
Minas Benyamin and Geoffrey H Goldman	
	5e. TASK NUMBER
	5f. WORK UNIT NUMBER

7. PERFORMING ORGANIZATION NAME(S) AND ADDRESS(ES)	8. PERFORMING ORGANIZATION REPORT NUMBER
US Army Research Laboratory Attn: RDRL-SES-P 2800 Powder Mill Road Aelphi, MD 20783-1138	ARL-TR-7086

9. SPONSORING/MONITORING AGENCY NAME(S) AND ADDRESS(ES)	10. SPONSOR/MONITOR'S ACRONYM(S)
	11. SPONSOR/MONITOR'S REPORT NUMBER(S)

12. DISTRIBUTION/AVAILABILITY STATEMENT
Approved for public release; distribution unlimited.

13. SUPPLEMENTARY NOTES

14. ABSTRACT

An analysis of detection and tracking performance for a Class I unmanned aircraft system (UAS) measured with a small tetrahedral microphone array was performed. Detection and tracking algorithms were implemented using beamforming and adaptive Kalman filters. The performance of a coherent energy-based detection algorithm implemented with a delay and sum beamforming algorithm was assessed using receiver operation characteristics (ROC) curves. Angle tracking was implemented using an adaptive Kalman filter with input from a filter and sum beamforming algorithm. For good signal-to-interference-plus-noise ratios (SINR), the estimated azimuth angles had good agreement with ground truth data, but the estimated elevation angles were underestimated inaccurately by a scale factor.

15. SUBJECT TERMS
acoustic UAV UAS analysis detection tracking

16. SECURITY CLASSIFICATION OF:			17. LIMITATION OF ABSTRACT	18. NUMBER OF PAGES	19a. NAME OF RESPONSIBLE PERSON Geoffrey H Goldman
A. Report	b. ABSTRACT	c. THIS PAGE	UU	34	19b. TELEPHONE NUMBER *(Include area code)*
Unclassified	Unclassified	Unclassified			301-394-0882

Standard Form 298 (Rev. 8/98)
Prescribed by ANSI Std. Z39.18

Contents

List of Figures

Acknowledgments

INTENTIONALLY LEFT BLANK.

1. Introduction

Small commercially available unmanned aircraft systems (UAS) can provide enemy forces with a low-cost reconnaissance and surveillance capability against US Soldiers in combat outposts (COPS) and forward operating bases (FOBS), potentially compromising their missions. Soldiers would like to negate this threat. If this is not feasible, Soldiers would like to know when they are being observed by a UAS and what information is being compromised. To address this need, the US Army is promoting the development of systems to detect, track, and classify small UAS with low size, weight, power, and cost (SWaP-C). Traditionally, radar and electro-optical systems have been used to track manned and unmanned aircraft, but many of these systems have high SWaP-C. An alternative approach is to use acoustic sensors that have low SWaP-C, but have smaller detection ranges compared to other high SWaP-C sensors. For many scenarios, this is a good trade-off. Additional detection range can potentially be achieved by placing acoustic sensors down range.

An array of microphones can be used to detect and estimate the direction of arrival (DOA) of sounds from sources such as UASs using beamforming algorithms. By triangulating with 2 or more microphone arrays, the location of the target can be estimated and tracked. By measuring the spectrum of the target, information about the type of UAS can be obtained. For this report, data from a single, small tetrahedral microphone array was analyzed. The array does not provide for optimal detection and tracking performance, but it can easily be folded up and carried in a Soldier's backpack, then placed at a FOB or COP.

A detection algorithm was implemented by comparing the coherent output of a conventional delay and sum beamforming algorithm to a threshold. This approach is not optimal, but it is a standard approach that will provide a baseline for performance against a Class I UAS.[3]

2. Measurements

Test data for a Class I UAS was gathered using the tetrahedral microphone array shown in Fig. 1. Four data runs were measured during a single day over a 5-h period. The acoustic data was sampled at 10 kHz. Global position system (GPS) data sampled at a rate of 1 Hz on the UAS.
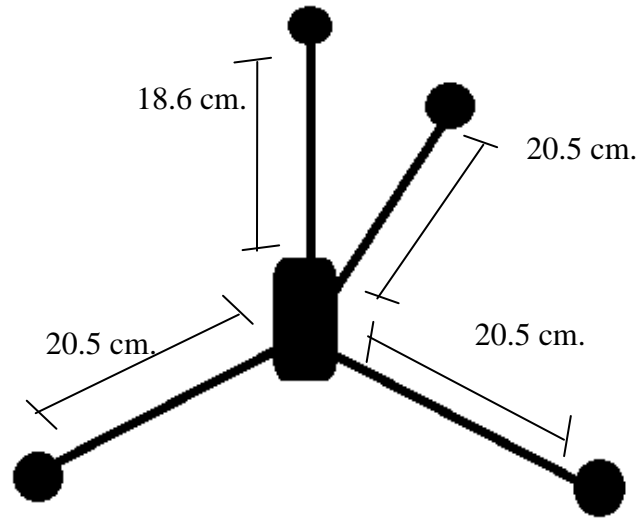
Fig. 1   Tetrahedral microphone array configuration

Microphone calibrations were taken at the test site, but due to an unspecified error, were lost and replaced by calibrations made at a different time, but using the same array. The data was multiplied by a scaling factor calculated using a 94 dB, 1024 Hz calibration tone. Figures 2 and 3 show typical spectrums of ambient noise and the UAS.
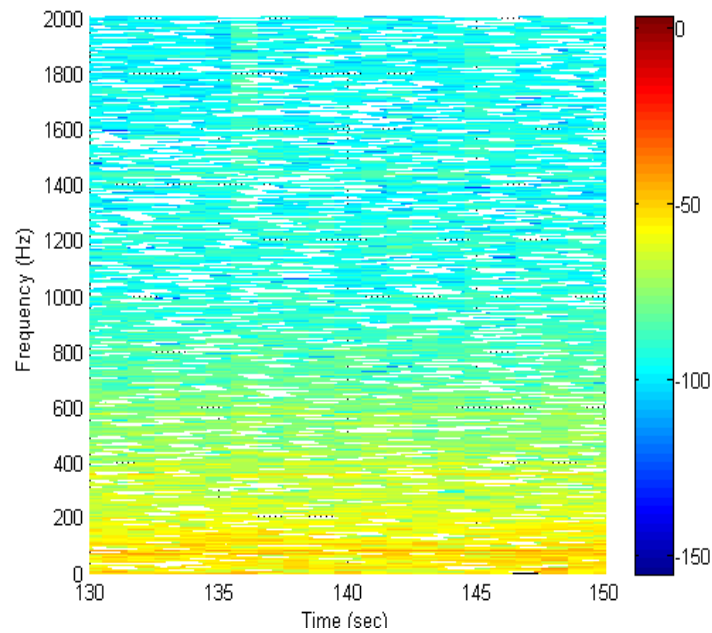

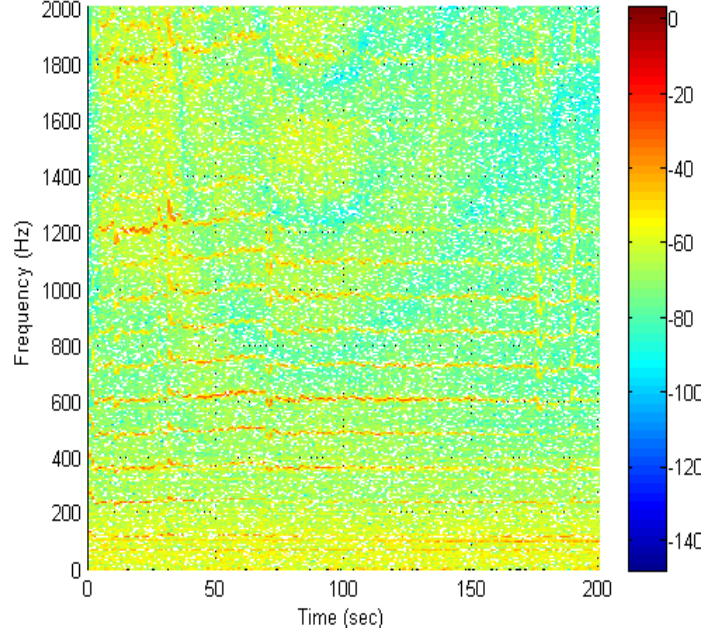Fig. 2   Spectrum of typical ambient noise

Fig. 3   Spectrum of the UAS

The received signal at each microphone can be modeled using

$$y(t) = \frac{s(t)}{r(t)^M} + \gamma(t)$$

(1)

where $y(t)$ is the received signal at a microphone, $s(t)$ is the signal from the source, $\gamma(t)$ is independent and zero mean noise, $r(t)$ is the range to the target, and M is a constant that is equal to 1 for spherical attenuation. The average power of the received signal can be modeled by squaring Eq. 1 to obtain

$$y(t)^2 = \frac{s(t)^2}{r(t)^{2M}} + E(\gamma(t)^2)$$

(2)

where E denotes expected value. Now, M can be estimated by taking the log of Eq. 3 and performing a linear regression. The results are shown for all 4 runs in Fig. 4.
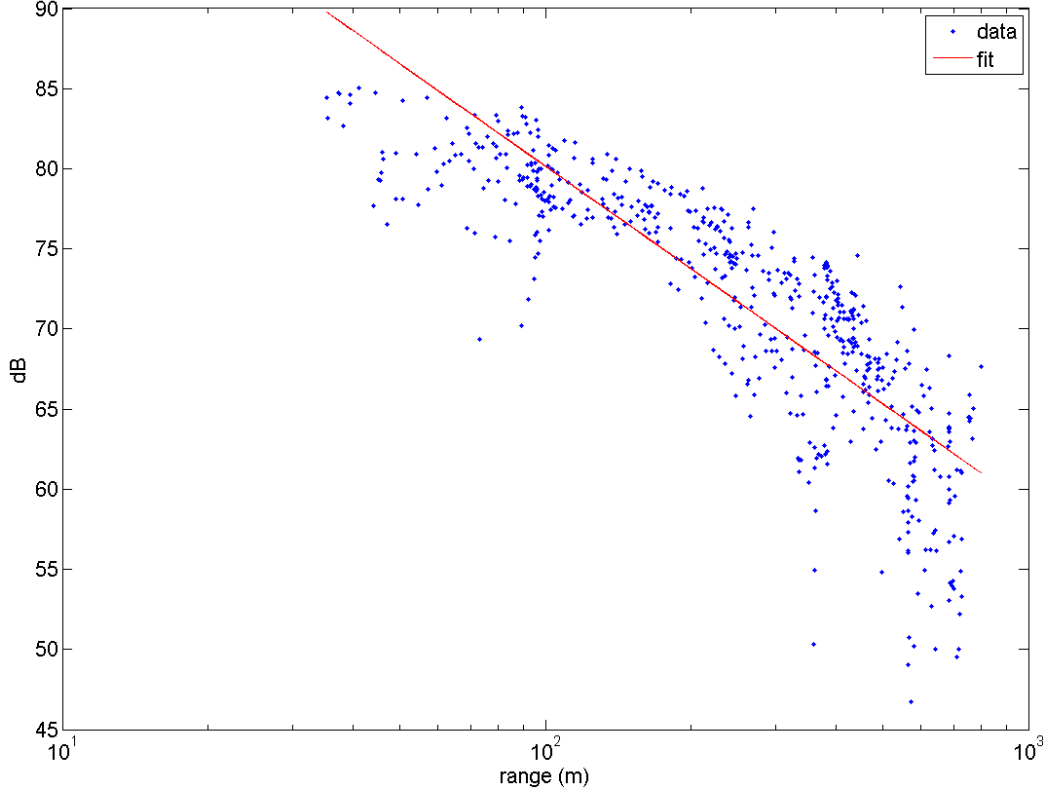
3

Fig. 4   Linear fit of the acoustic power as a function of range

The slope of the line is –2.12, which corresponds to M=1.056. These results indicate that the attenuation of the signal is primarily due to spherical spreading.

3.   Signal Processing

Beamforming algorithms have been successfully implemented in numerous applications to detect and track targets using a coherent array of sensors. A standard approach is the delay and sum beamformer algorithm, which estimates the direction of arrival (DOA) by maximizes the coherent power calculated using

$$\int_{T} y(t)^2 \, dt \tag{3}$$

where

$$y(t) = \sum_{I} x_i(t - \tau_i)\omega_i \tag{4}$$

$$\tau_i = -\frac{\vec{a}'p_i}{c}, \tag{5}$$

$x_i(t)$ is the signal measured on the ith sensor, T is the integration time, τ_i is a fixed time delay, ω_i is a weight, $\vec{a}$ is the direction of arrival of a signal in the far-field traveling towards the sensor array, pi is the sensor location, $'$ denotes transpose, and c is the propagation speed.[1]

The beamformer can be further improved by compensating for channel effects on each signal using

$$y(T) = \int_T \left(\sum_I \left(\int x_i(t - \tau_i - r)h_i(r)dr \right) \right)^2 \omega_i dt, \tag{6}$$

where $h_i(r)$ is a weighting function. A standard weighting function is based upon a Wiener filter.[2] For beamforming algorithms that are implemented in the frequency domain, the Fourier transform of the weighting can be calculated using

$$H(\omega) = \frac{P_{ss}(\omega)}{P_{ss}(\omega) + P_{nn}(\omega)}, \tag{7}$$

where $P_{ss}(\omega)$ is the power spectral density of the signal and $P_{nn}(\omega)$ is the power spectral density on the noise. For independent signals and noise measured with matched microphones, $H(\omega)$ can be estimated using

$$H(\omega) \approx \frac{\sum_I |Y_i(\omega)|^2 / I - P_{nn}(\omega)}{\sum_I |Y_i(\omega)|^2 / I}, \tag{8}$$

when $\sum_I |Y_i(\omega)|^2 / I > P_{nn}(\omega),$

otherwise $H(\omega) = 0$,

where $Y_i(\omega)$ is the Fourier transform of yi(t).

The weighting function was estimated using the noise power spectrum calculated over 4-s intervals using all the noise data. Figure 5 shows the average power spectrum of the noise.
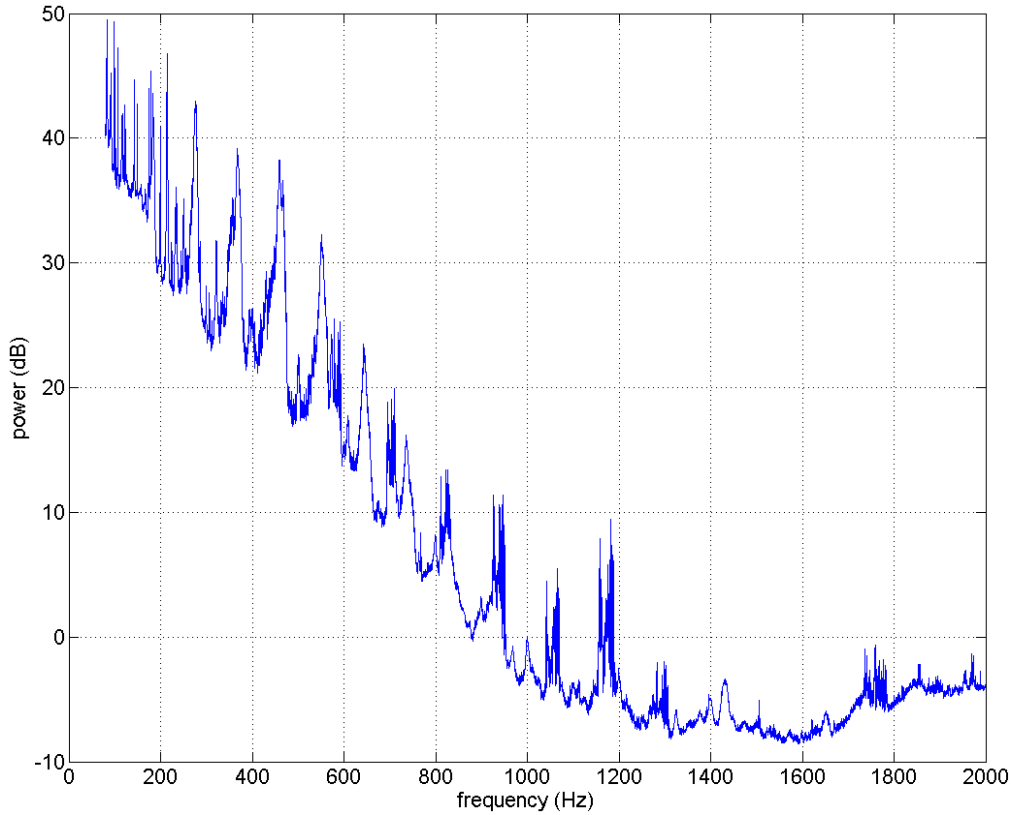
5

Fig. 5   Average power spectrum of the ambient noise

4.   Detection Performance

Receiver operating characteristics (ROC) curves are used to describe the performance of a binary detection algorithm. They show the probability of false positive rate versus the probability of detection. The detection algorithm is based upon the coherent energy from a delay and sum beamforming algorithm exceeding a threshold. The data are processed over non-overlapping 4-s intervals.

The data used to generate the ROC curves can be visualized by comparing histograms of the signal against histograms of the signal plus noise. The histograms of the noise were calculated from the power of the delay and sum beamformer signal when there was no target present for several frequency bands of interest and at several angles. The results were calculated at an elevation angle of $\pi/2$ and azimuth angles of 0, $\pi/2$, π, and $3\pi/2$ radians for each frequency band of interest. The histograms of the signal plus noise were only calculated when the azimuth tracking algorithm had locked onto the UAS. This requirement reduced the probability of signals from other targets in the vicinity artificially increasing the energy estimates for the UAS plus noise. Results from the tracking algorithm are presented in the tracking algorithm section.

6

ROC curves were generated using data measured with the tetrahedral microphone array over 4 different runs on the same UAS at 4 different range intervals. Acoustics data were preprocessed with 4 different band-pass filters implemented with a rectangular window in the frequency domain. The first bandpass filter was between 80 to 2000 Hz. The output of the beamforming algorithm was used to generate histograms of the noise and signal plus noise, as shown in Figs. 6 and 7. These data were used to generating ROC curves in Fig. 8.
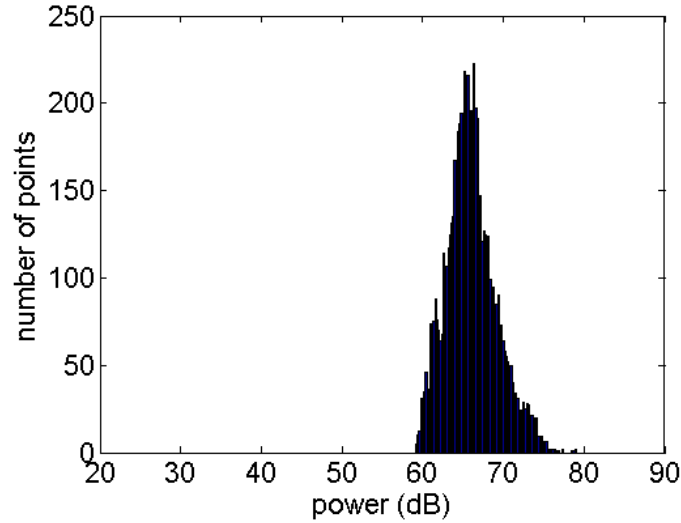

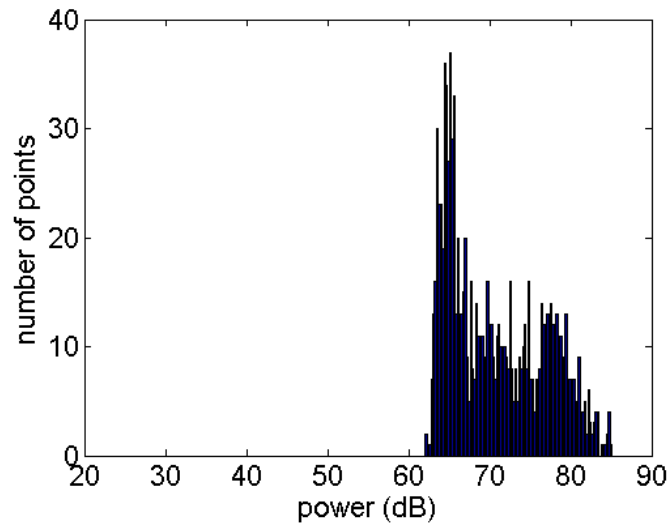Fig. 6   Noise histogram for band-pass filter between 80 to 2000 Hz

Fig. 7   Signal plus noise histogram for band-pass filter between 80 to 2000 Hz
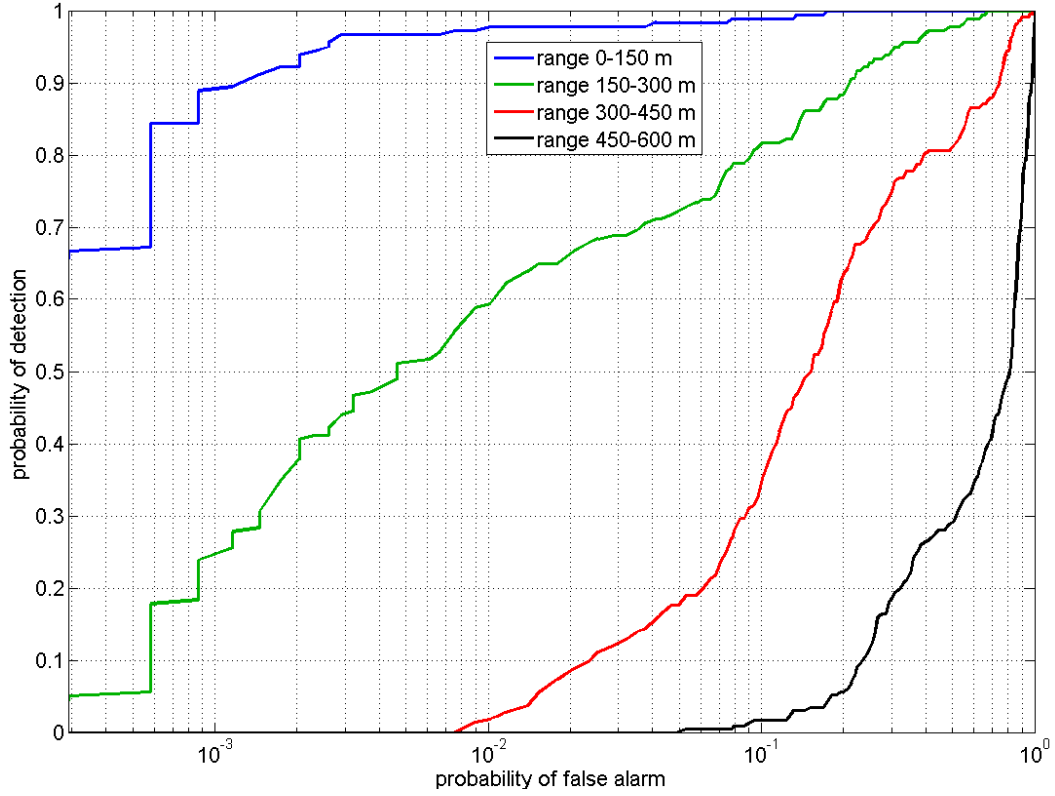
Fig. 8 Roc curves for band-pass filter 80 to 2000 Hz

Next, a bandpass filter between 250 and 2000 Hz was used to preprocess the data. The resulting histograms of the noise and signal plus noise are shown in Figs. 9 and 10, and the resulting ROC curves are shown in Fig. 11.
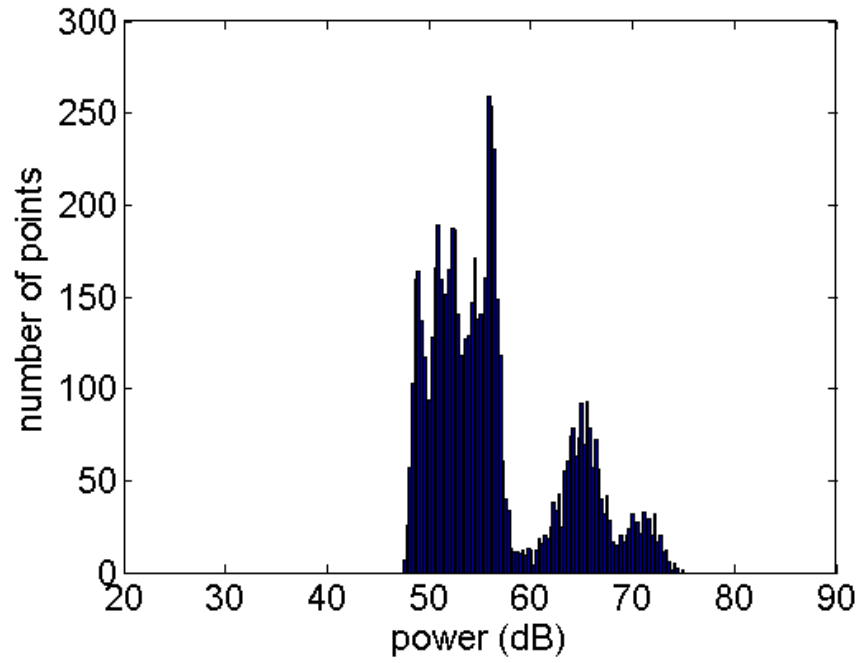
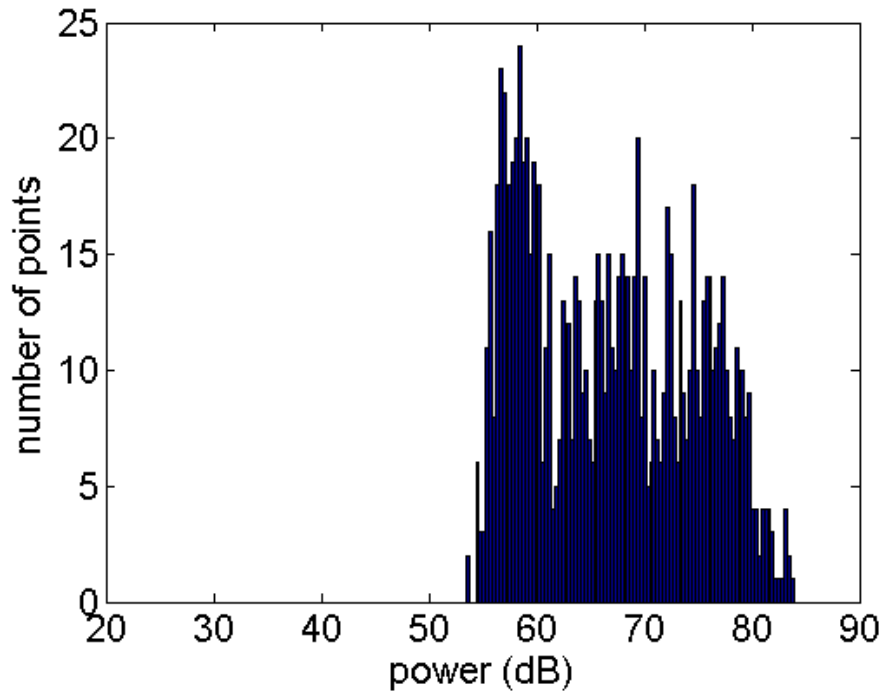Fig. 9   Noise histogram for band-pass filter 250 to 2000 Hz

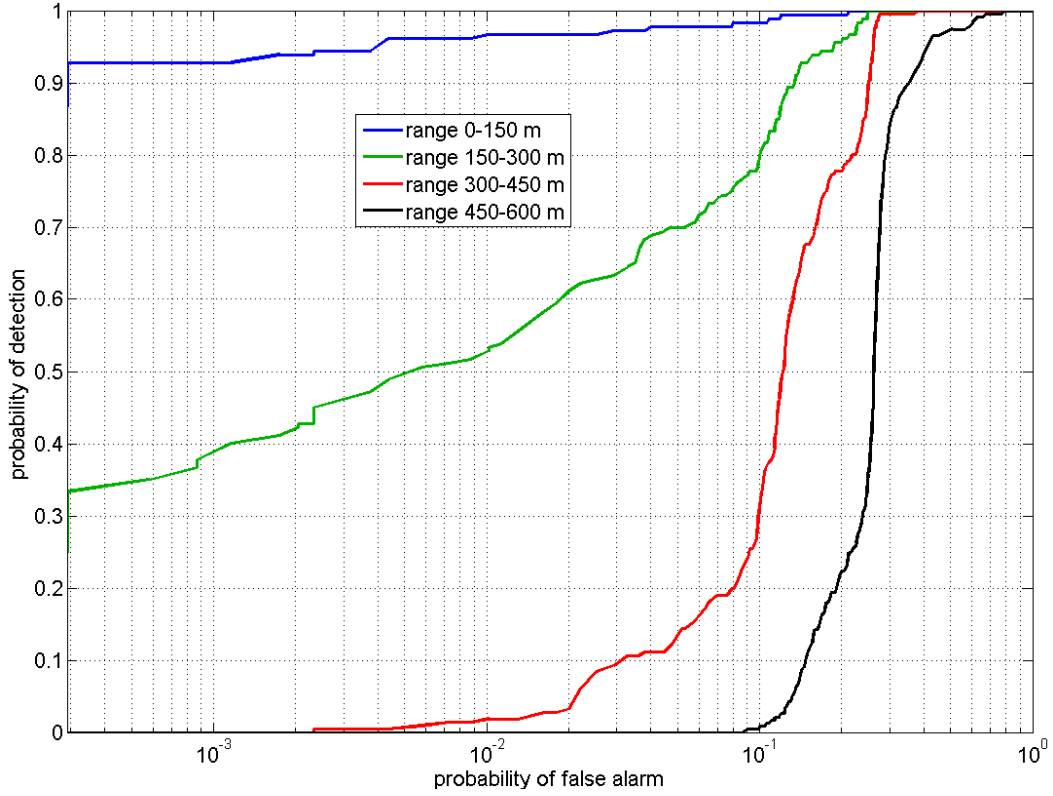Fig. 10   Signal plus noise histogram for band-pass filter 250 to 2000 Hz

Fig. 11   Roc curves for band-pass filter 250 to 2000 Hz

Next, a bandpass filter between 400 and 2000 Hz was used to preprocess the data. The resulting histograms of the noise and signal plus noise are shown in Figs. 12 and 13, and the resulting ROC curves are shown in Fig. 14.
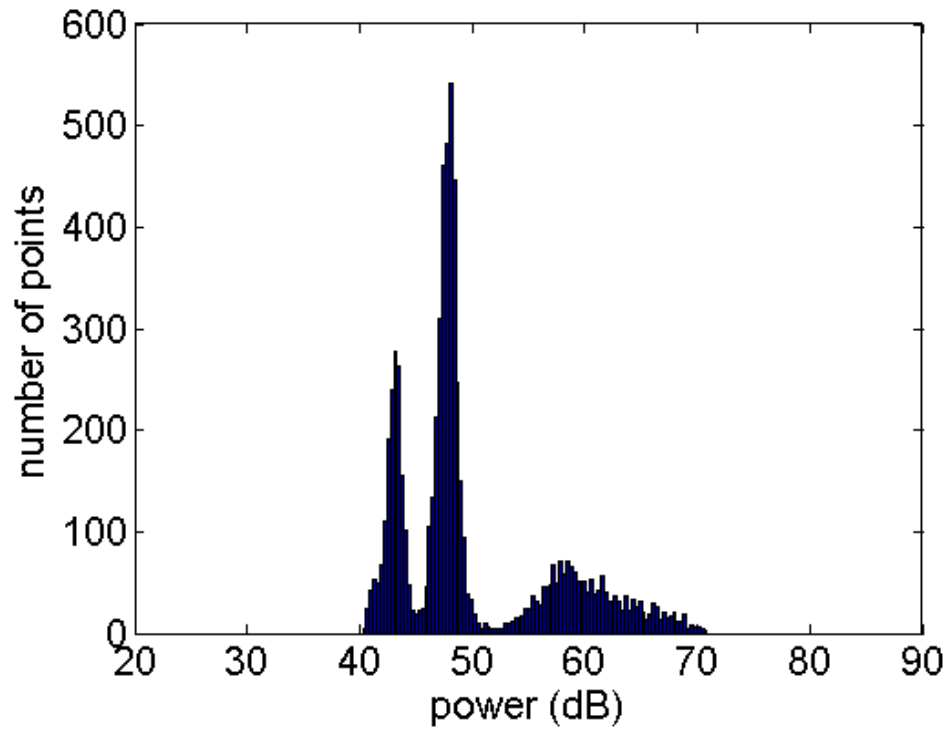
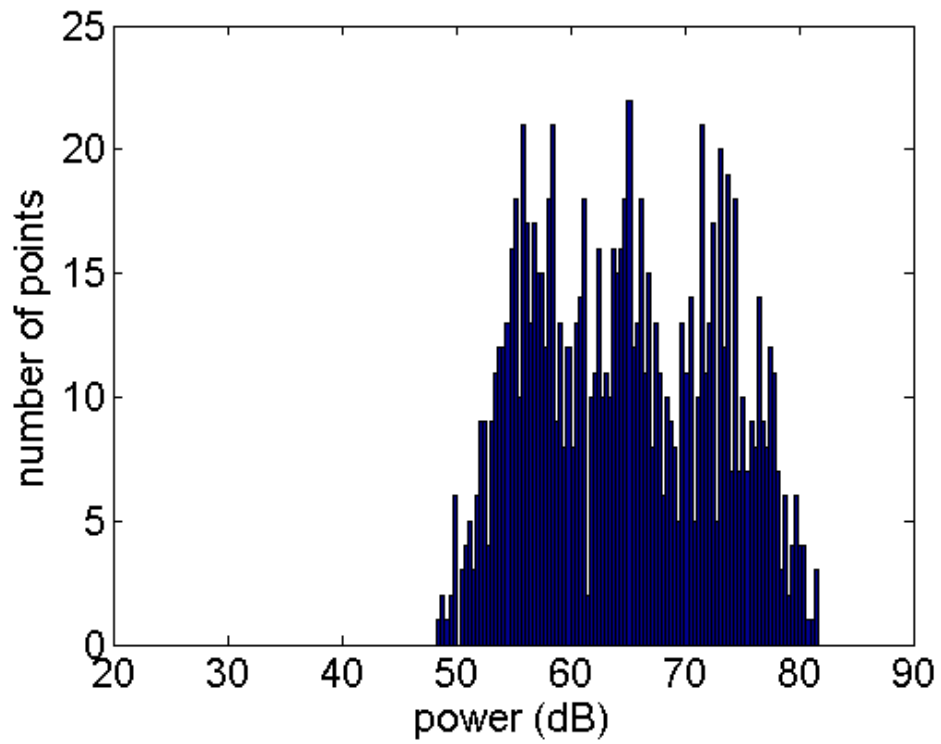Fig. 12   Noise histogram for band-pass filter 400 to 2000 Hz

Fig. 13   Signal plus noise histogram for band-pass filter 400 to 2000 Hz
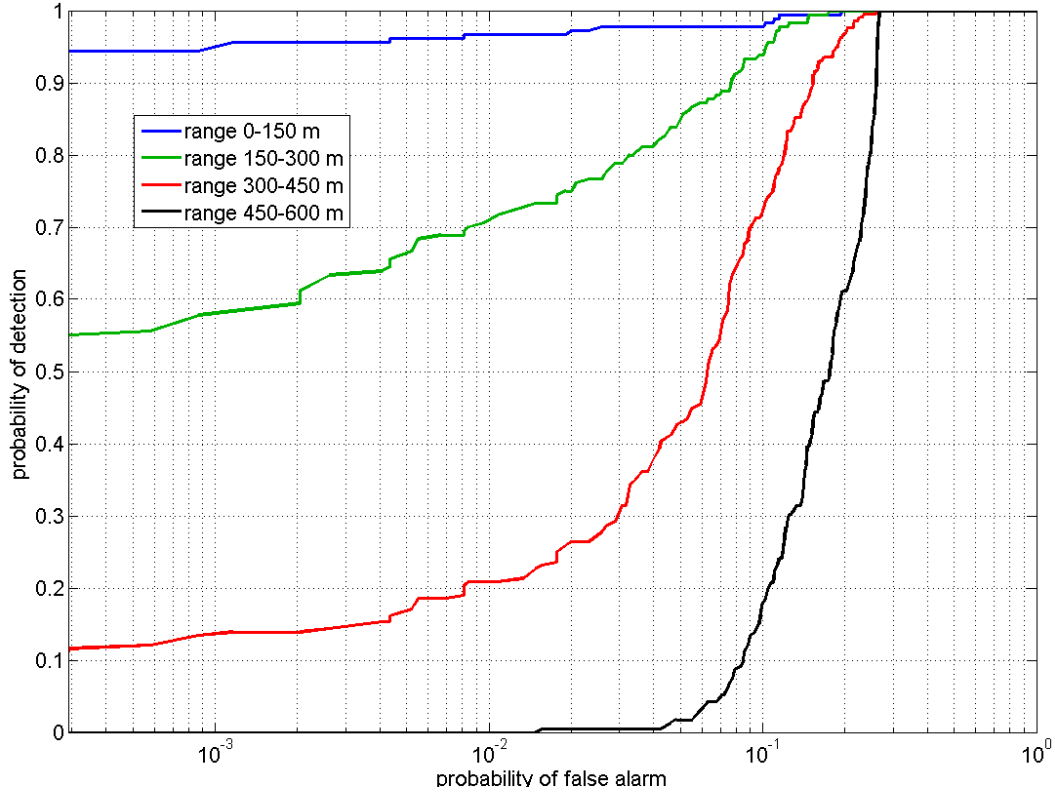
11

Fig. 14 Roc curves for band-pass filter 400 to 2000 Hz

Next, a bandpass filter between 800 and 2000 Hz was used to preprocess the data. The resulting histograms of the noise and signal plus noise are shown in Figs. 15 and 16, and the resulting ROC curves are shown in Fig. 17. The narrowest frequency interval had the best results.
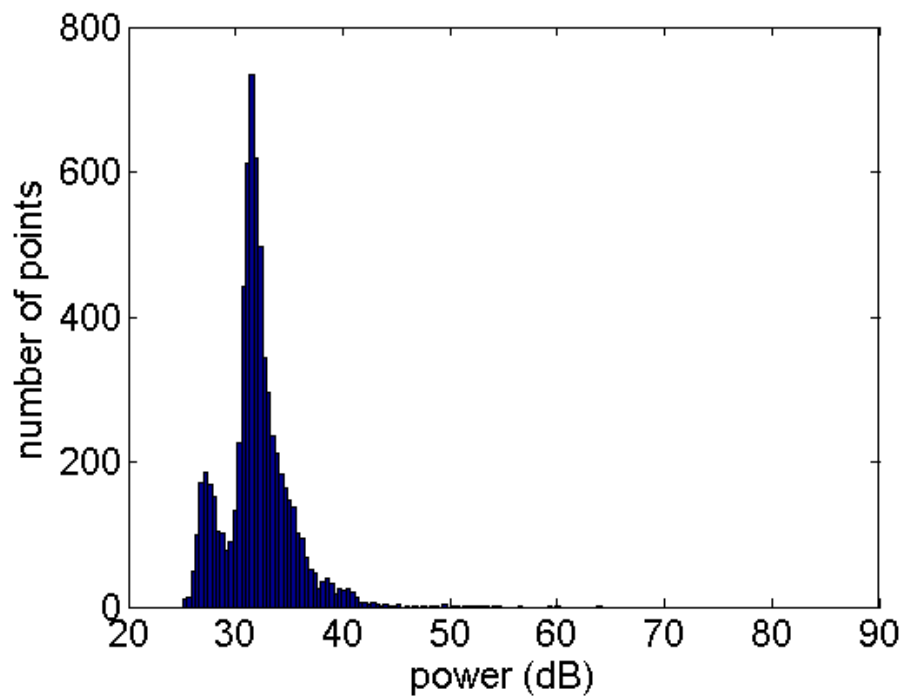
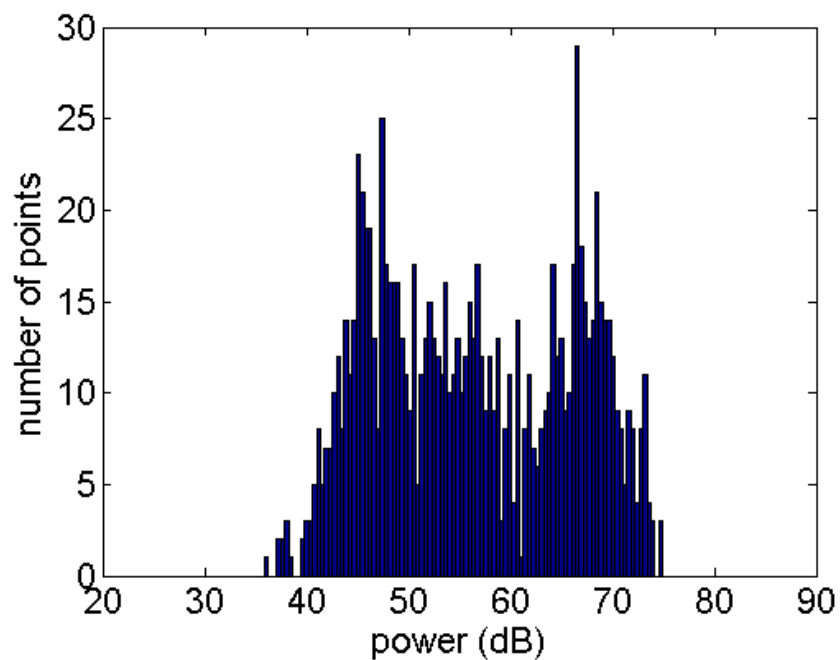Fig. 15　Noise histogram for band-pass filter 800 to 1700 Hz

Fig. 16　Signal plus noise histogram for band-pass filter 800 to 1700 Hz
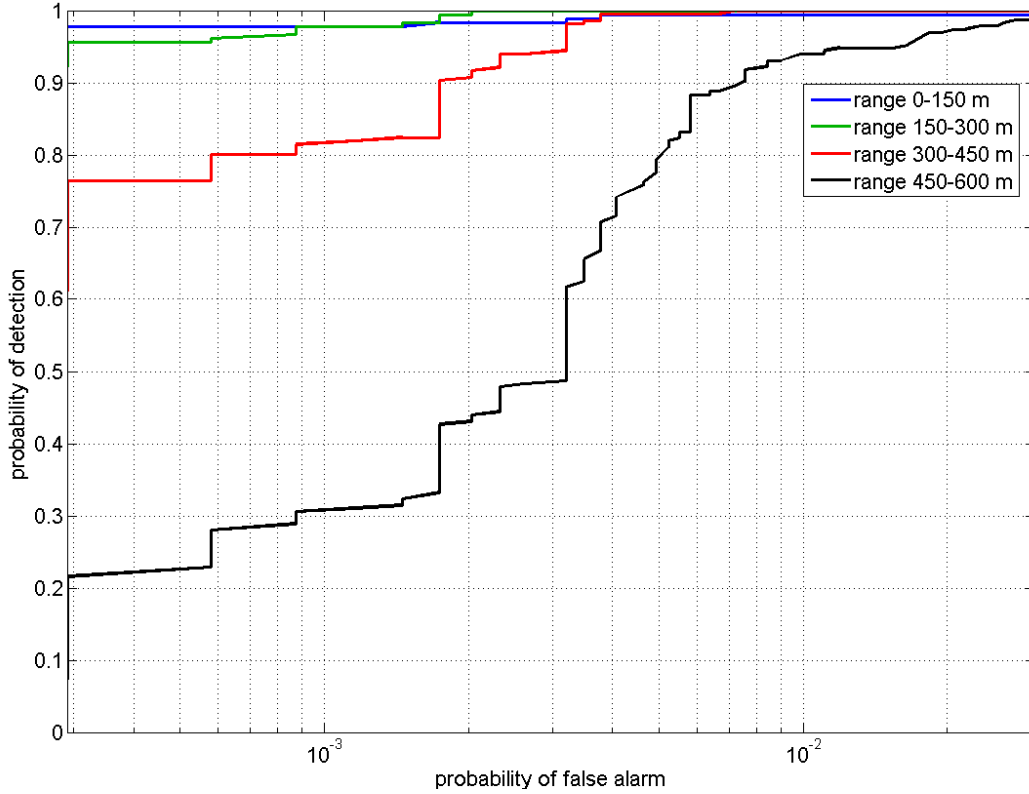
13

Fig. 17   Roc curves for band-pass filter 800 to 1700 Hz

The detection algorithm with data filtered from 800–1700 Hz had a 99.5% probability of detection for ranges less than 450 m, with a 0.3% false alarm rate compared to a 95% probability of detection with a 10% false alarm rate (Fig. 14). The detection performance increased at the farthest ranges, as well giving a 99% probability of detection for the UAS ranging from 450–600 m with a 3% false alarm rate. The previous performance shown in Fig. 14 was a 95% probability of detection with a 25% false alarm rate.

The increased performance with the more restrictive frequency ranges can be explained by examining the histograms of the noise and the signal plus noise. Reducing the frequency range of the data slightly reduced the values of the signal plus noise, but it had a large effect on reducing the values of the noise.

5.   Angle Tracking

The UAS was tracked in the azimuth and elevation angles using input from a filter and sum beamformer that was filtered using an adaptive Kalman filter.[4] The beamforming algorithm used estimates of the noise shown in Fig. 5 to calculate weighting functions using Eq. 7. Results are

14

shown for each of the 4 runs. First, the azimuth angle tracking results are shown for the first UAS flight in Fig. 18. The range of the UAS is included on the right side of the y-axis.
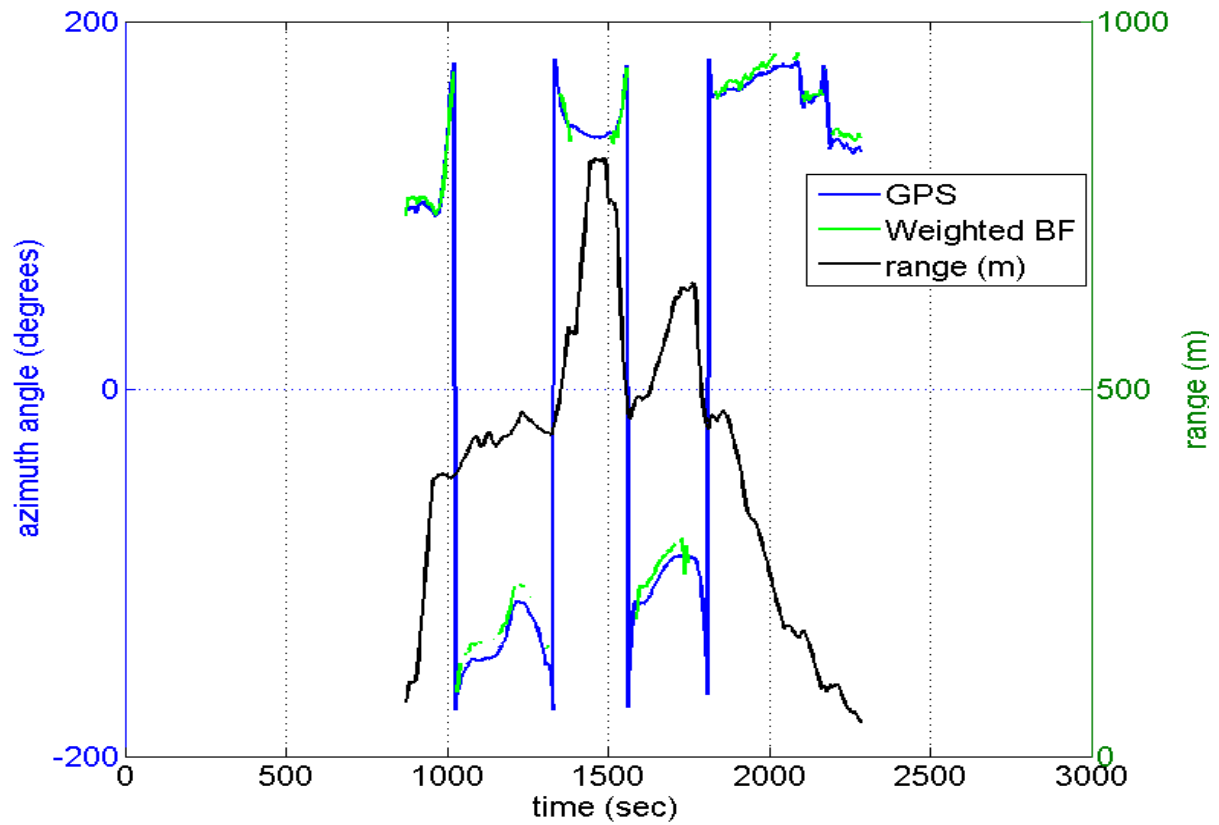

Fig. 18   Azimuth angle tracking flight I

The predicted azimuth angle tracking was close to the GPS calculations for the first flight. The range varied between 0 and 800 m. There were no other known targets in the scene. The second UAS flight is shown in Fig. 19.
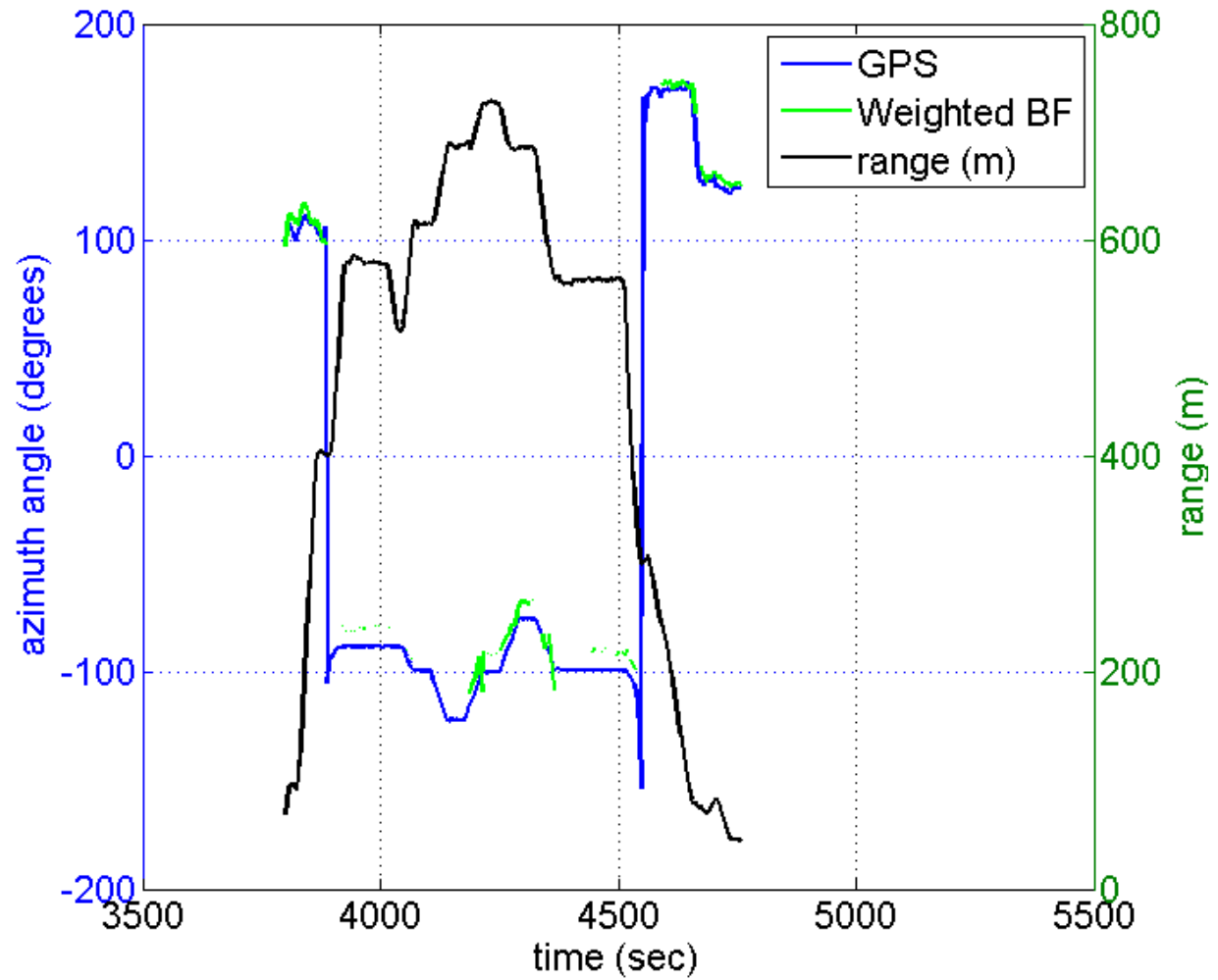
Fig. 19　Azimuth angle tracking for flight II

The tracking accuracy was poorer for flight II due to the presence of a helicopter, which interfered with the angle estimation for the UAS. This occurred again during the third flight, which degraded the tracking performance, as seen in Fig. 20.
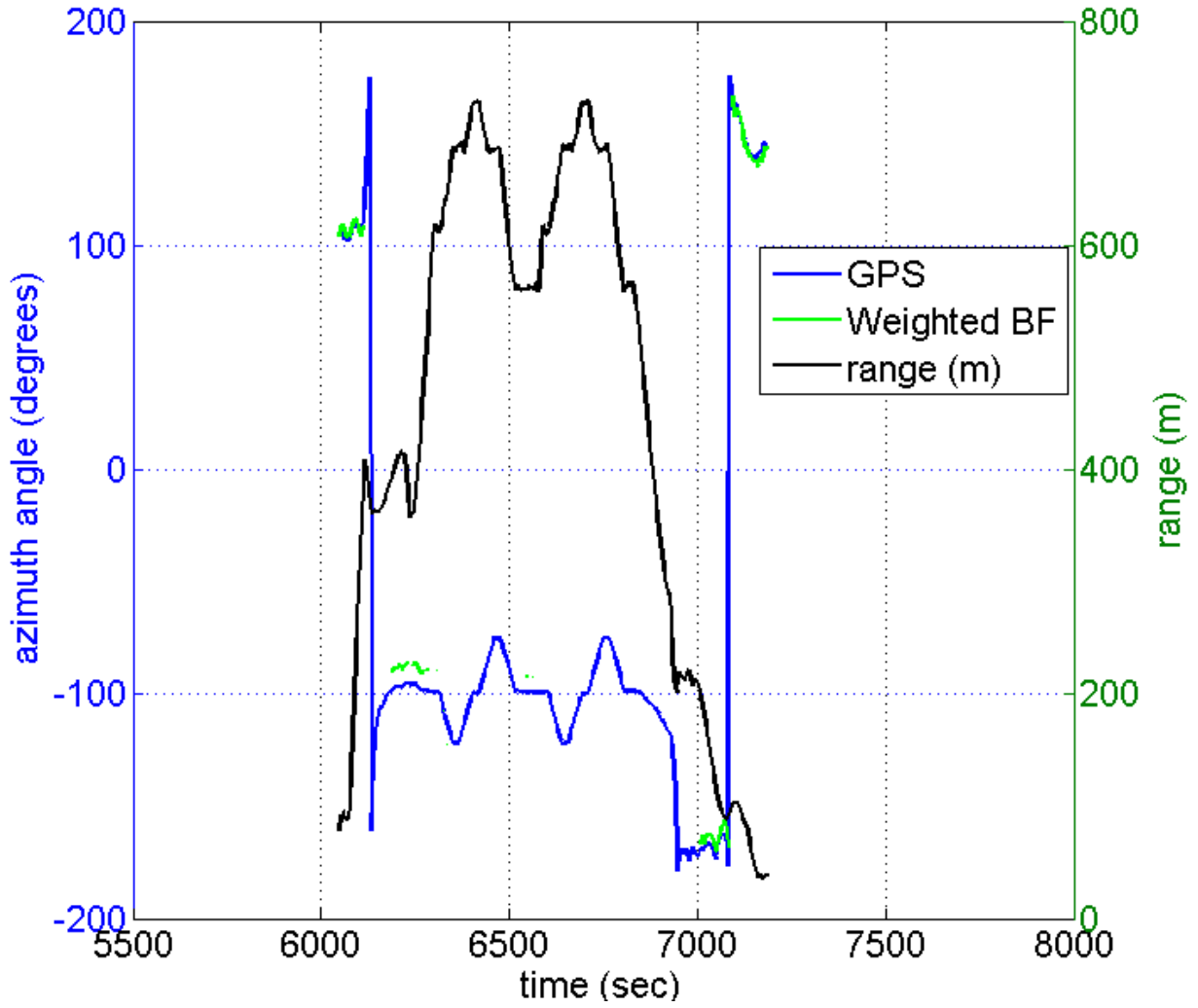
Fig. 20   Azimuth angle tracking flight III

Flight III had the worst tracking performance of the 4 runs. Despite limiting the look angle of the beamformer, which aided it into locking onto the UAS, the previously tracked target, the strong signal of a helicopter interfered with the signal of the UAS. Flight IV showed the best tracking results, with almost complete agreement with the ground truth, as shown in Fig. 21.
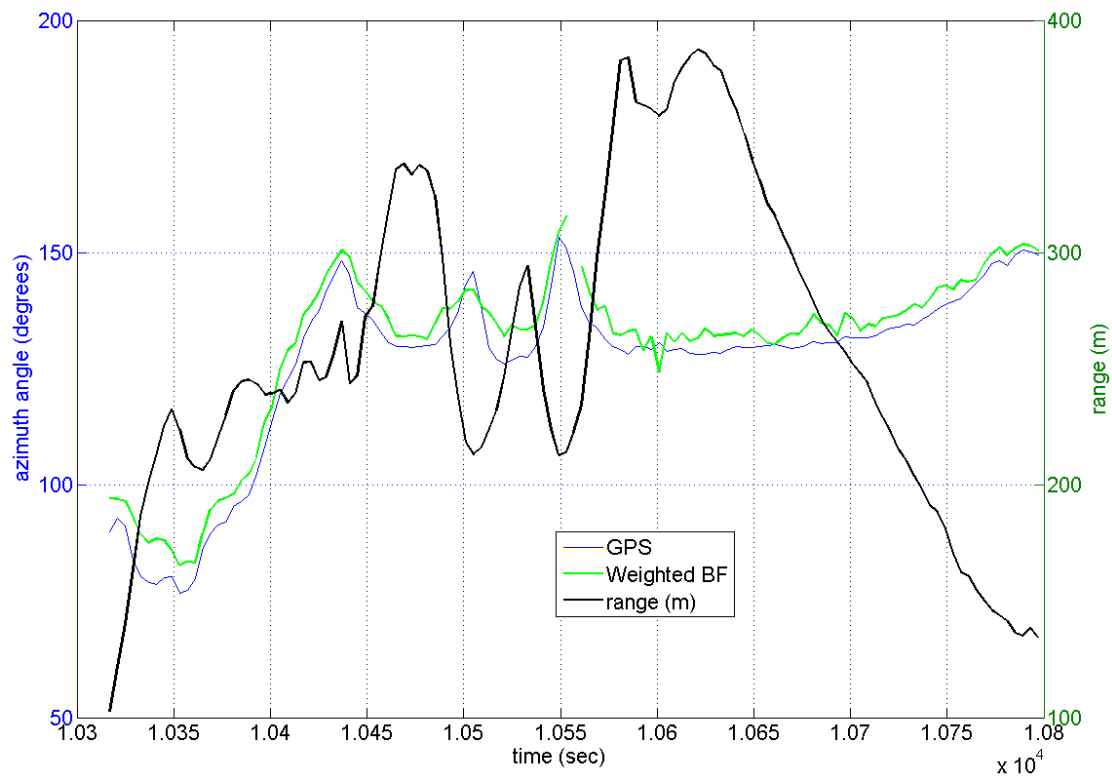
Fig. 21   Azimuth angle tracking flight IV

Elevation angle tracking results were also processed and compared to ground truth data for the 4 flights. Figures 22–25 show the results for the 4 flights.
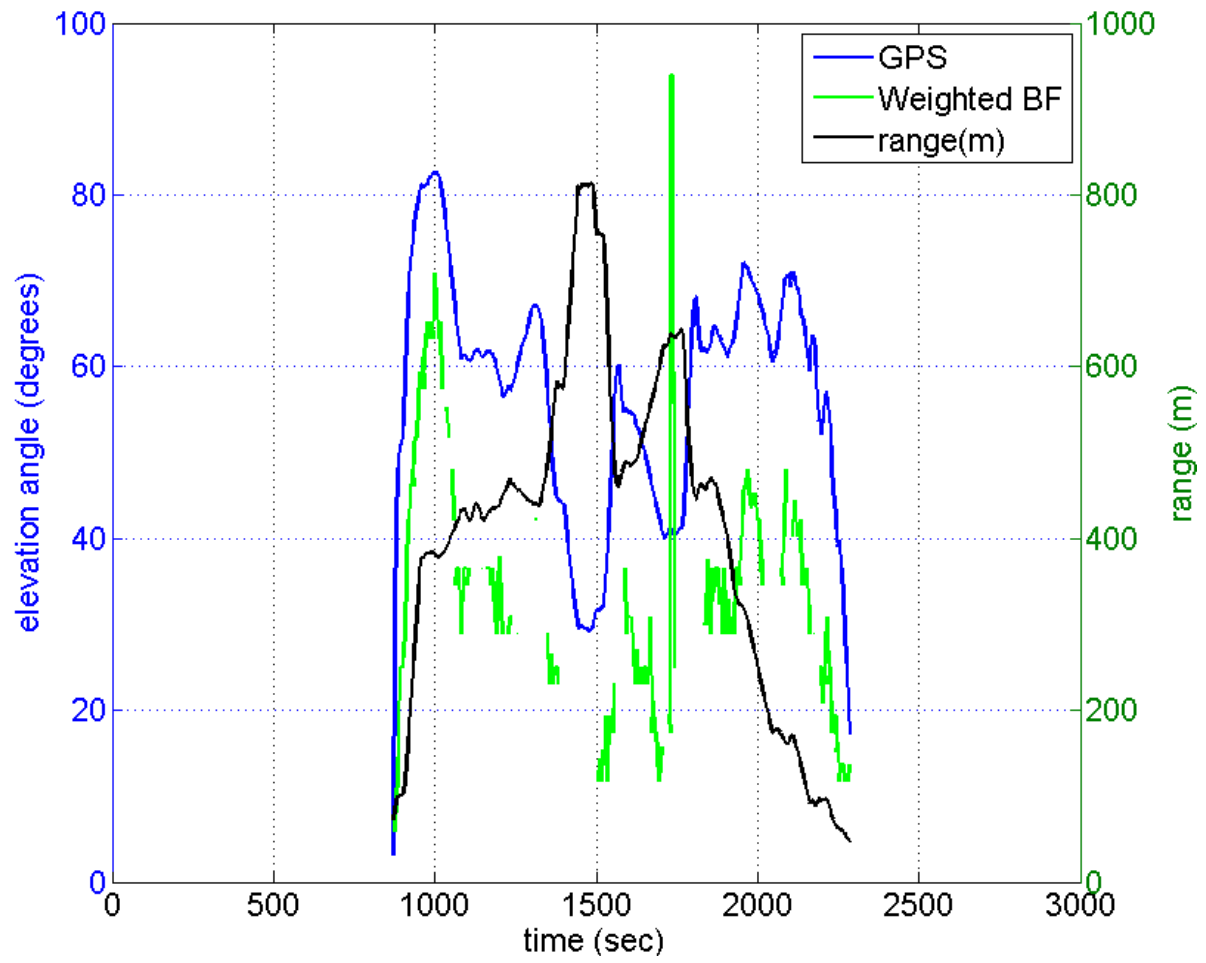
Fig. 22   Elevation angle tracking results for flight I
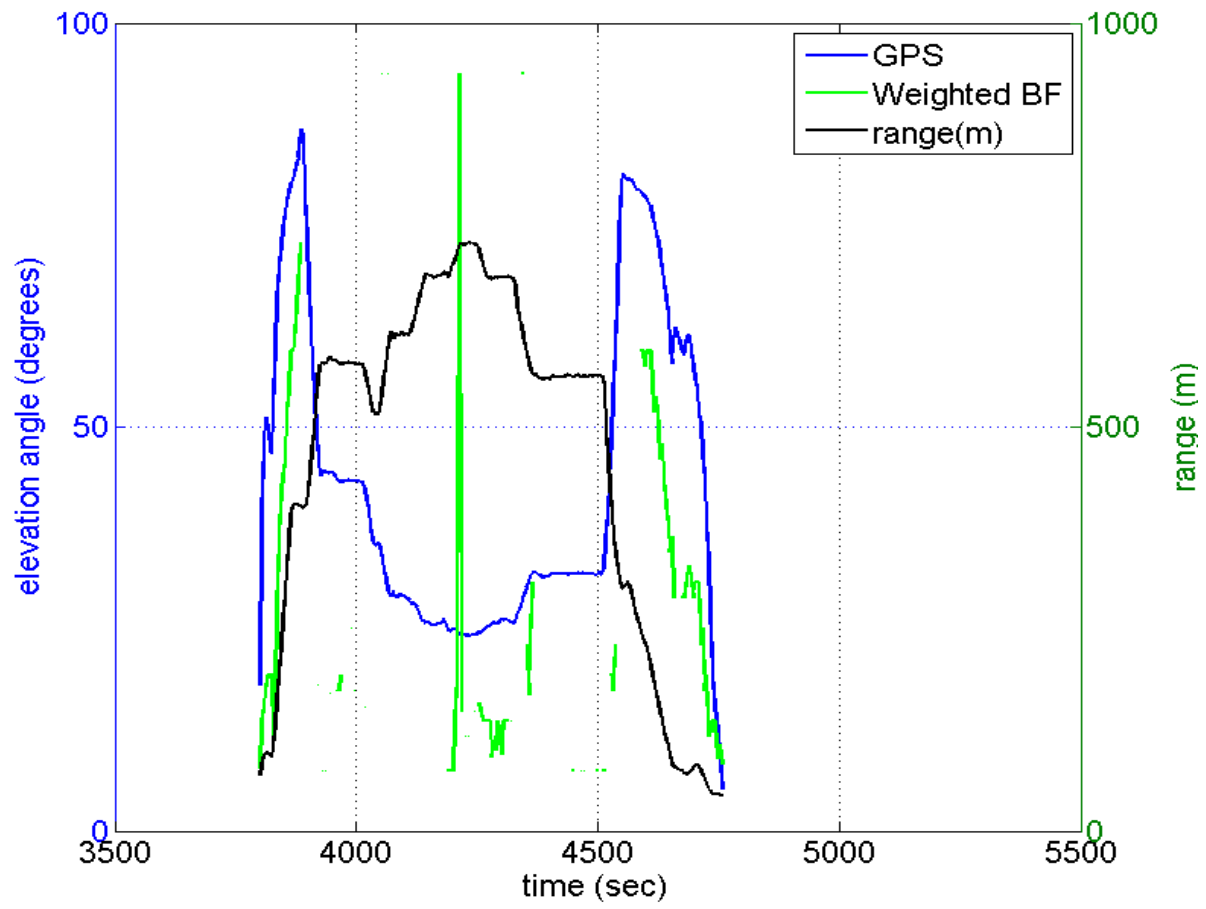
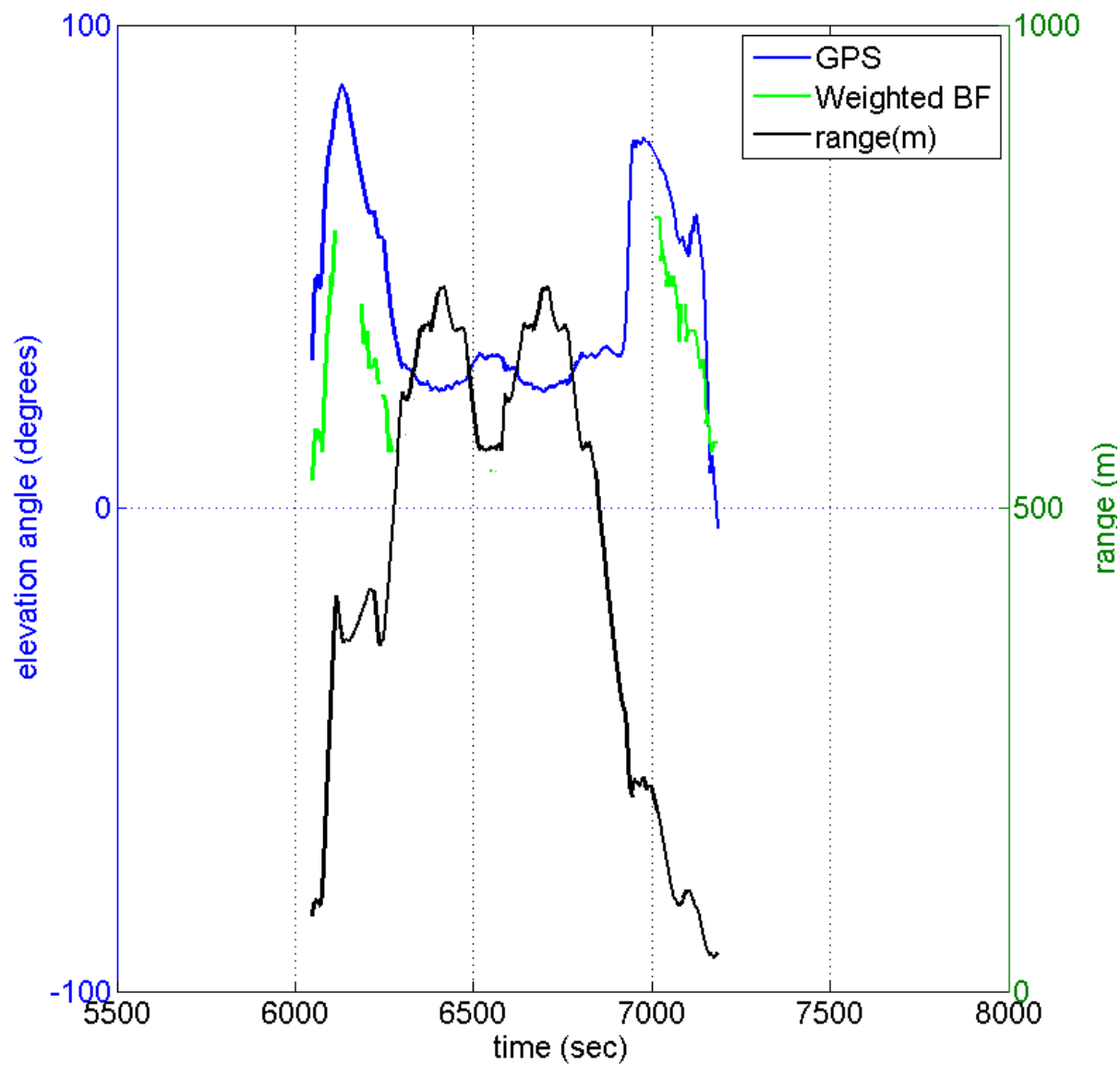Fig. 23   Elevation angle tracking results for flight II

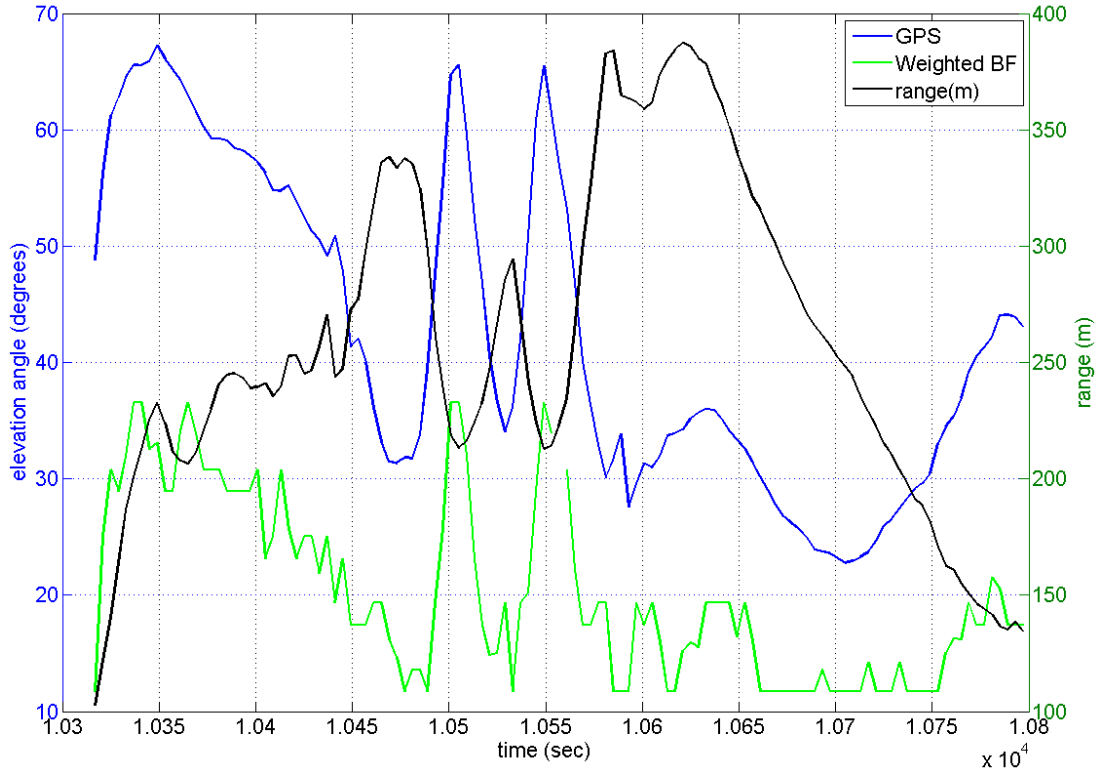Fig. 24   Elevation angle tracking flight III

Fig. 25   Elevation angle tracking results for flight IV

The elevation angle tracking results appeared to have offset and scaling issues. Overall, the elevation tracking results improved at higher elevations relative to lower ones. Poor elevation tracking results appear to be somewhat correlated with range, but only loosely since poor performance occurs everywhere.

6.   Conclusion

An acoustic systems analysis of detection and tracking performance for a Class I UAS measured with a small tetrahedral microphone array was performed. Detection and tracking algorithms were implemented using an adaptive Kalman filter with input from a beamforming algorithm. The performance of a coherent energy-based detection algorithm implemented with a delay and sum beamforming algorithm was assessed using ROC curves. The detection algorithm had the best performance with a passband of 800–1700 Hz with a 99.5% probability of detection at ranges below 600 m and a 3% false positive rate. Detection algorithm results should be improved by using a filter and sum beamformer rather than a delay and sum beamformer, but it would require a much more sophisticated simulation to estimate the performance.

The tracking angle results were mixed. Despite constraining the look angle of the beamforming algorithm, the tracking algorithm often lost track when other targets were present. When the

22

tracking algorithm reacquired the track, it was often tracking a helicopter, rather than the UAS. Overall, azimuth tracking was adequate, following the GPS over 60% of the time within a 10° margin.

The elevation tracking results were poor. There appeared to be an offset and scaling error associated with the elevation angle estimates. This may be likely the result of using a standard beamforming algorithm, rather than using an algorithm that incorporated a ground bounce into the calculation.

7.   References

1.   Johnson DH, Dudgeon DE. Array signal processing: concepts and techniques. Prentice Hall, 1993.

2.   Nilsen CC, Holm S. Wiener beamforming and the coherence factor in ultrasound imaging. Ultrasonics, Ferroelectrics and Frequency Control. IEEE Transactions on 57.6. 2010;1329–1346.

3.   Kay SM. Fundamentals of statistical signal processing: estimation theory.Prentice-Hall, 1993.

4.   Goldman GH. Adaptive angle-of-arrival estimation and tracking algorithm for rotorcrafts. in Proceedings of MSS BAMS, Oct 2012. (FOUO)

5.   Mucci FA. A comparison of efficient beamforming algorithms. IEEE Trans on Acoasr, Speech, Signal Processing. Jan. 1984;32(3): 548–558.

1 (PDF)	DEFENSE TECHNICAL INFORMATION CTR DTIC OCA
1 (PDF)	GOVT PRINTG OFC A MALHORTA
1 (PDF)	DIRECTOR US ARMY RESEARCH LAB IMAL HRA MAIL & RECORDS MGMT
1 (PDF)	DIRECTOR US ARMY RESEARCH LAB RDRL CIO LL
2 (PDS)	DIRECTOR US ARMY RESEARCH LAB RDRL SES P C YANG G GOLDMAN
6 (PDS)	US ARMY RSRCH LAB ATTN ATTN RDRL SES P M SCANLON ATTN RDRL SES P M TENNEY ATTN RDRL SES P M TRAN-LUU ATTN RDRL SES P M ALBERTS ATTN RDRL SES S G WILLIAMS ATTN RDRL SES S R HOLBEN
4 (PDS)	US ARMY ARDEC FUZE PRECISION ARMAMENT TECHNOLOGY DIV ATTN A MORCOS ATTN H VANPELT ATTN J CHANG ATTN S DESAI

INTENTIONALLY LEFT BLANK.